PROCEEDINGS, 45th Workshop on Geothermal Reservoir Engineering
Stanford University, Stanford, California, February 10-12, 2020
SGP-TR-216

A Preliminary Investigation on the Cost Reduction Potential of Optimizing Bore Fields for Commercial Ground Source Heat Pump Systems

Jeffrey D. Spitler[1], Jack C. Cook[1], Xiaobing Liu[2]

[1]School of Mechanical and Aerospace Engineering, Oklahoma State University, Stillwater, OK 74078

spitler@okstate.edu

[2]Oak Ridge National Laboratory, Oak Ridge, TN 37831

liux2@ornl.gov

Keywords: ground source heat pump, vertical bore ground heat exchanger, cost reduction

ABSTRACT

The high initial cost of ground heat exchangers (GHE) is a primary hurdle preventing wider adoption of ground source heat pump (GSHP) systems. GHEs used for commercial GSHP systems commonly consist of vertical boreholes installed on a grid with equal spacing between boreholes. Significant thermal loads require a large number of boreholes to be present in the field. However, due to thermal interactions among boreholes, the ground formation in the center of a bore field can, over time, become thermally saturated when the thermal load is not balanced on an annual basis. The loss of effectiveness due to thermal saturation at the center boreholes in regularly spaced borehole fields suggests that larger spacing near the center of the bore field could be more optimal, and in return reduce initial costs. Through computer simulations using the latest development of a GHE modeling tool, this study evaluates the impacts of various unconventional designs of the borehole field on the performance and cost of the GHEs of a typical commercial GSHP system. The unconventional designs include irregular spacing among boreholes with decreased spacing around the perimeter and increased spacing in the interior of the field. The unconventional bore field design shortens the total drilling length by up to 42% while giving better heat transfer performance than a conventional bore field design. The significant total bore length reduction is due to improved heat transfer effectiveness of each borehole in the unconventional bore field.

1. INTRODUCTION

It was estimated that residential and commercial buildings contributed 40% of all United States energy consumption in 2011, 43% of which can be attributed to heating, ventilation, and air conditioning (HVAC) (D&R International 2012). This implies that approximately 17% of the total energy consumption in the United States is a result of residential and commercial HVAC systems. Energy efficient alternatives to conventional HVAC technology are desired to reduce this energy consumption and the associated greenhouse gas emissions. The ground source heat pump (GSHP) is an energy efficient technology for space heating, cooling and air conditioning. Approximately 1758 TWh (6 quadrillion BTUs) of primary energy can be saved annually in the United States by retrofitting existing heating and cooling systems with GSHPs (Liu et al. 2019). The high efficiency of GSHPs is a result of the favorable subsurface temperature of the ground, which is cooler than ambient air in summer but warmer than ambient air in winter. However, the adoption of GSHPs in the United States is currently limited by their high cost of installation. The ground heat exchanger (GHE), which is used to exchange heat with the surrounding ground formation, accounts for about 30% of the total installation cost of a GSHP system (NYSERDA 2017). The most commonly used GHE in the United States for commercial GSHP systems is the vertical bore ground heat exchanger (VBGHE), and the expensive drilling required to create the borehole is the primary factor contributing to the high cost of VBGHE installation (Liu et al. 2018).

VBGHEs used for commercial GSHP systems usually consist of many vertical boreholes to meet the thermal demands. Conventional designs of VBGHEs usually layout boreholes in regular grids and fix the spacing and depth of boreholes. Bayer et al. (2014) reported that the number and total length of boreholes can be reduced by strategically placing boreholes in an irregular pattern, as illustrated in Fig. 1. This strategy results in uniform heat transfer within a bore field by removing the less effective boreholes, which are usually located in the center of a bore field and which can become thermally saturated over time.

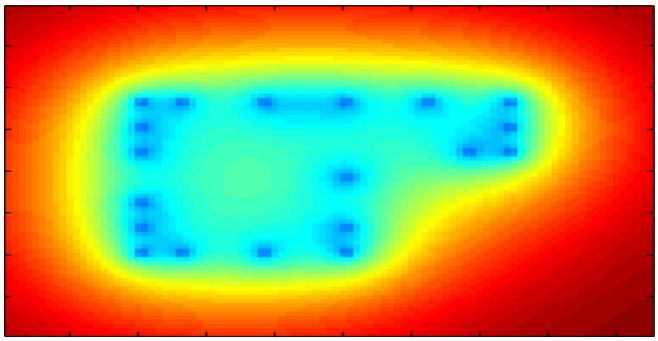

Figure 1. Temperature distribution of a strategically optimized bore field by Bayer et al. (2014). Used by permission.

Most existing commercial design tools for VBGHE rely on libraries of pre-computed response functions known as g-functions. Use of these libraries precludes unconventional designs, such as irregular spacing among boreholes, different depths and inclination angles of boreholes in a bore field. It thus limits the capability of these design tools for identifying an optimal bore field design that can be implemented with less drilling and associated costs.

This paper presents a study of several conventional and alternative bore field designs using a new VBGHE simulation tool. The cost reduction potential is evaluated by comparing the total drilling lengths resulting from the different bore field designs under the same loading and geological conditions.

2. METHODOLOGY

Temperature response functions, known as g-functions, are a computationally efficient method for simulating VBGHEs either as part of a whole-building energy simulation, or as part of a dedicated GHE design tool. At present, they are the only feasible way to simulate a VBGHE of a ground source heat pump system in a whole-building energy simulation (Mitchell and Spitler 2019) with a speed that may be acceptable in the context of simulating the building. The g-functions represent the response of the ground heat exchanger; pre-calculation of this response is what allows the computational time to be as low as it is. At the time of their development, the original g-functions (Claesson and Eskilson 1985) were computed with a numerical method. The implementation of this numerical method is not publicly available. As a result, GHE design tools are often limited to configurations that were computed by Eskilson (1986) or later by Hellström for the Earth Energy Designer program (BLOCON 2019).

A number of researchers have looked at alternate methods for computing g-functions. Cimmino and Bernier (2014) presented a new method for calculating g-functions, which uses superposition of an analytical solution of "stacked" finite-line-sources to compute the response of a multi-borehole ground heat exchanger. That is, each borehole is divided into multiple segments, each represented by a finite line-source. One of the key difficulties in this or any method is determination of the distribution of heat over the boreholes. Cimmino (2019a) refined the approach and has also released it (Cimmino 2019b) as an open source project called "pygfunction."

In this study, Cimmino's pygfunction is used to generate g-functions for several conventional and alternative bore field designs, and the bore depth of each bore field design is sized for meeting the thermal load of a GSHP system. The resulting total borehole lengths for maintaining the supply water temperature of the VBGHE within a specific range are compared to determine cost reduction potential of alternative bore field designs.

2.1 G-function Generator

Cimmino (2019a; 2019b) made significant speed improvements in solving the integral involved in the analytical solution of the finite line source presented by Claesson and Javed (2011). To further increase the calculation speed, Cimmino (2019a; 2019b) identifies the symmetries within a borehole field and only computes segment-to-segment response factors for each unique pair of segments. The method, as implemented in pygfunction, determines the required time-varying heat flux on each segment under a given boundary condition, such as uniform borehole wall temperature (UBHWT) or uniform inlet fluid temperature (UIFT). In this paper, we utilize the UBHWT boundary condition with six segments per borehole to compute the g-functions. Arguably, the UIFT boundary condition most closely matches the physical situation. However, our experience (Spitler and Cook 2019) has been that using the UBHWT boundary condition with six segments gives g-functions that match very well the UIFT with many (12) segments. Historically, the pygfunction implementation utilized a description of the ground heat exchanger in the Python code. That is, to compute a g-function, the Python code would be edited and the results of pygfunction were presented by plotting or printing to the console. The original pygfunction code was adapted in this study so that the inputs and outputs are file-based, and it can be readily scripted to calculate g-functions of both conventional and unconventional bore fields.

The accuracy of pygfunction has been verified by comparing its results for bore fields with regular spacing to the long-time g-functions provided by Eskilson (1986) and used in the GLHEPRO program (Spitler 2000; OSU 2016). Figure 2 shows comparisons of the g-functions generated with pygfunction for the cases with 100-144 boreholes. The dashed lines represent the g-functions used by GLHEPRO. For typical ground thermal properties at Atlanta, GA (k=2.423 W/(m·K); ρc_p= 2343.493 kJ/(K·m^3)) and a borehole depth of 110m, these g-functions cover times from 3 days to 830 years. At $\ln(t/t_s)$ = -0.497, corresponding to 25 years, the differences between

the g-functions in the GLHEPRO library and those computed with pygfunction are about 1%. This implies that for the worst case of a completely imbalanced system with a constant load on the GHE, the prediction of long-term temperature rise or fall at the borehole wall could be off by about 1% after 25 years. This error is much smaller than other errors in the design process and is therefore acceptable.

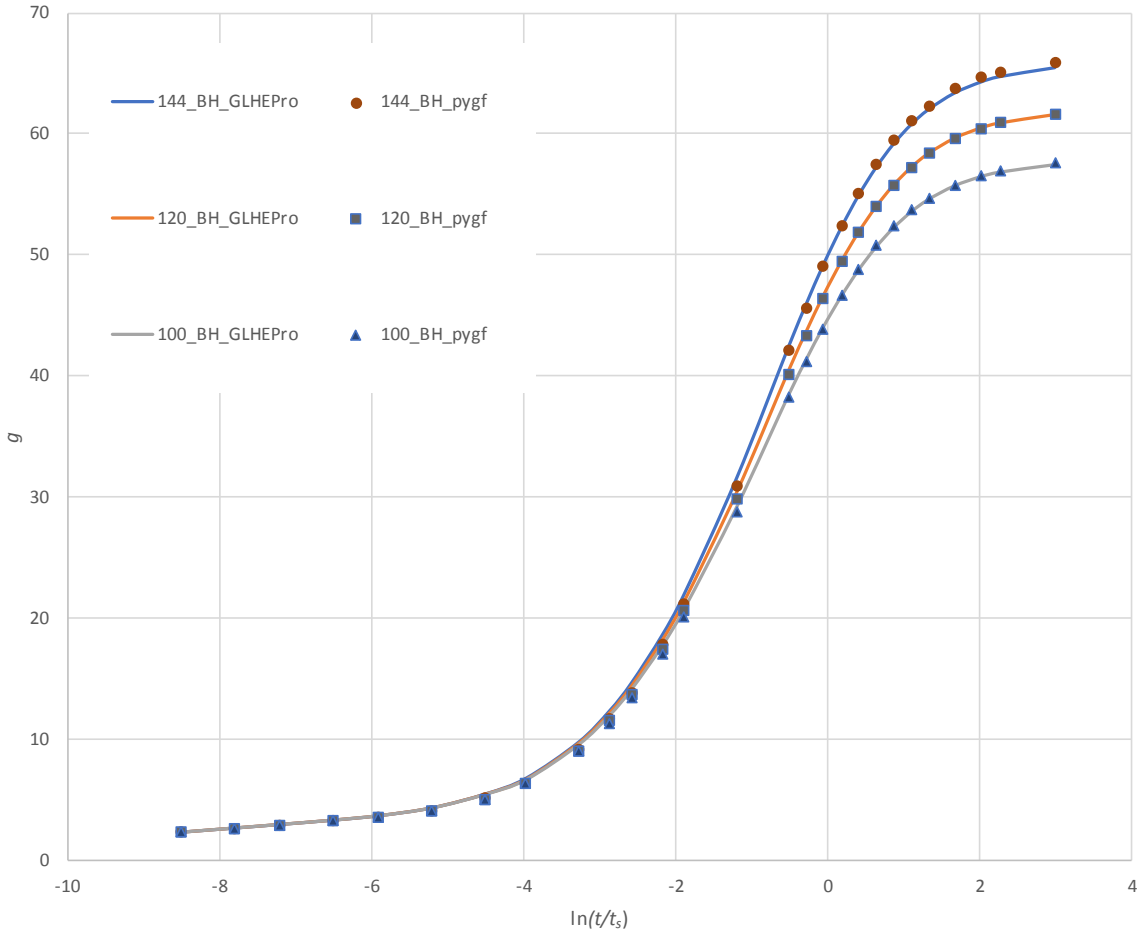

Figure 2 Comparisons between g-functions computed with pygfunction and GLHEPRO .

2.2 GSHP System Simulation

In this study, the computer model of a medium-size office building from the U.S. Department of Energy's Commercial Reference Building Models (Deru, et al. 2011) is used to represent a common office building under typical operation. The modeled office building has three stories and a total floor area of 4,995 m^2 (53,600 ft^2). A 3-dimensional (3-D) image of the modeled office building is shown in Fig. 3. This building has a rectangular footprint with a length of 50 m (163.8 ft) and a width of 33.3 m (109.2 ft).

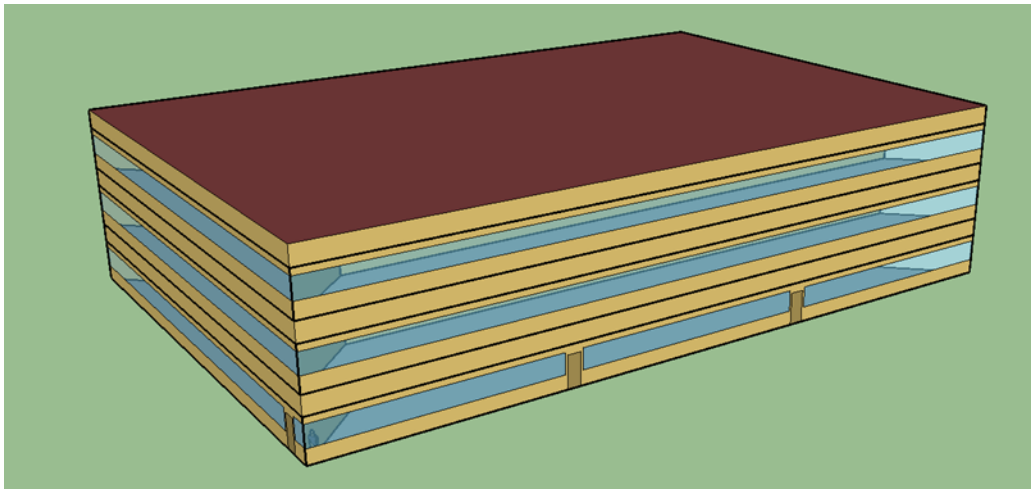

Figure 3. A 3-D image of the modeled medium-size office building.

The GSHP system for this building uses a VBGHE and a distributed heat pump system, which is made up of multiple small packaged water-to-air heat pump units, each providing climate control to an individual zone of the building. All the heat pump units are connected to the VBGHE through a common two-pipe water loop. A pressure-controlled variable-speed pump is used to adjust the flow rate in the water loop based on the operation of the heat pump units. The heat pump units modeled in this study use two-stage compressors, which run at a low or high stage in response to the fluctuating space heating and cooling demands of the building. The nominal cooling and heating efficiencies (evaluated with the coefficient of performance, COP) at full capacity of the modeled two-stage GSHP unit are 5.3 (18.2 EER) and 4.0, respectively.[1] A dedicated outdoor air system (DOAS) continuously conditions about 2900 L/s of OA[2] to the design room temperature and delivers the air to each thermal zone in the building when it is occupied. The DOAS uses a special water-source heat pump (WSHP) unit that is also connected to the VBGHE. The GSHP system is decoupled from the OA ventilation and runs only to satisfy the thermostat requirements in each of the thermal zones in the building. The VBGHE is sized to be able to maintain its leaving fluid temperature (LFT) in the range between 35°C and 7.2°C over a 20-year period. For this office building in Atlanta, only the upper limit constrains the design. A 30-year design period was also investigated. The general trends shown in this paper are the same, regardless of the design period, though the required borehole depths are higher with a 30-year design period than with a 20-year design period.

2.3 Sizing

For each bore field configuration, the borehole depth is adjusted in order to meet but not exceed the maximum design leaving fluid temperature (35°C) of the GHE, which is the heat pump entering fluid temperature (HP EFT). The simulation uses the long-term g-functions generated with pygfunction and short-term g-functions calculated with GLHEPRO using the method of Xu and Spitler (2006). The reason for using the short-term g-functions generated by GLHEPRO is that they give an effective borehole wall temperature, that, when coupled with a steady-state model of the effective borehole thermal resistance, gives the correct mean fluid temperature. Other approximations may be needed for very short time-steps, but for sizing the ground heat exchanger, we do not use time steps of less than an hour, and this simple approximation is accurate at hourly time steps.

The simulation is performed with a hybrid time step approach (Cullin and Spitler 2011) that can run a 20-year simulation of a VBGHE in a fraction of a second. To avoid lengthy computation time for generating g-functions during the iterative sizing process, five sets of g-function data pairs for a given bore field with various bore spacing to depth ratios are pre-calculated with pygfunction and stored in a library. Lagrange polynomials are used to interpolate between the stored g-functions, to give the g-function corresponding to a specific borehole depth.

3. CASE STUDY

A case study was performed to investigate the advantages of alternative designs of VBGHE to those typically available in existing design programs. A medium-size office building in Atlanta was chosen for this study. The thermal loads on the VBGHE are calculated using the computer simulation described in Section 2 and plotted in Fig. 4. As expected for an office building in Atlanta, the system rejects much more heat to the ground than it extracts. In fact, the ratio of annual heat rejection to annual heat extraction is 23.5. We

---

1 The COP and EER are measured at AHRI/ISO/ASHRAE/ANSI 13256-1 rating conditions: for cooling at full capacity, with 25°C entering water temperature and 19°C web bulb entering air temperature; for heating at full capacity, with 0°C entering water temperature and 68°F dry bulb entering air temperature. The EER value of 8.2 is dimensionless. In common American units, the value is 27.9 (Btu/h)/W.

2 Calculated using the size of the simulated building, the occupancy density described in ASHRAE Standard 62.1-2004 (ASHRAE 2004b), and the ventilation requirement specified in ASHRAE standard 1999 (ASHRAE 1999).

thus expect long-term heat build-up in the ground around the ground heat exchanger, and the ground heat exchanger design must account for this.

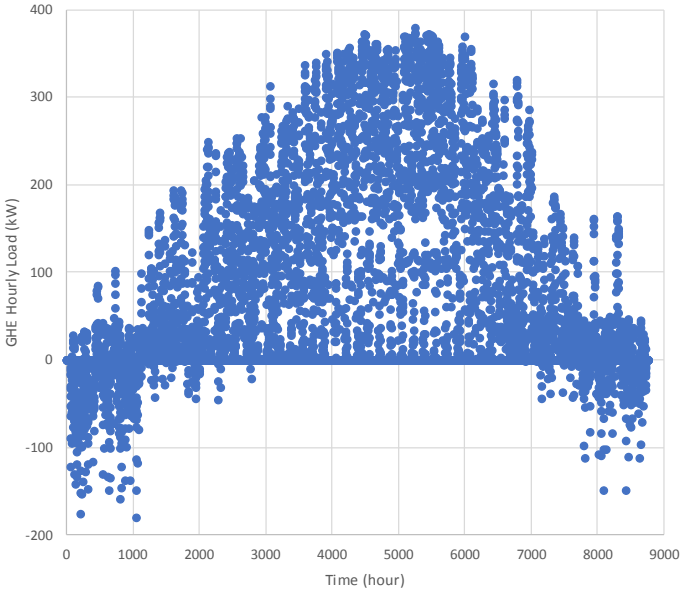

Figure 4. Hourly thermal loads of the ground heat exchanger (calculated with the DOE prototype model at Atlanta, GA).

As shown in Fig. 5, the building (in red) is set on a lot that is 70.1m x 80.8m. The undisturbed ground temperature is 18.3ºC and the ground thermal conductivity is 2.2 W/(m-K). A base case design with a 16x9 rectangular grid of 144 boreholes can fit into the available land in front of the building. The boreholes are regularly spaced on a grid of 4.6 m. To meet the design maximum entering fluid temperature (EFT) of 35°C for a 20-year design period, the required borehole depth is 110.1 m with a total borehole length of 15,853 m. This case is denoted "Base Case 1"; for reasons that will be explained below, a second base case, "Base Case 2", is also defined. Base Case 2 has 91 boreholes; for the same maximum EFT and design period, the required borehole depth is 135.0 m and the total borehole length is 12,283m.

The bore size is determined iteratively by simulating the leaving fluid temperature of the bore field with various bore depths in response to the thermal loads of the VBGHE.

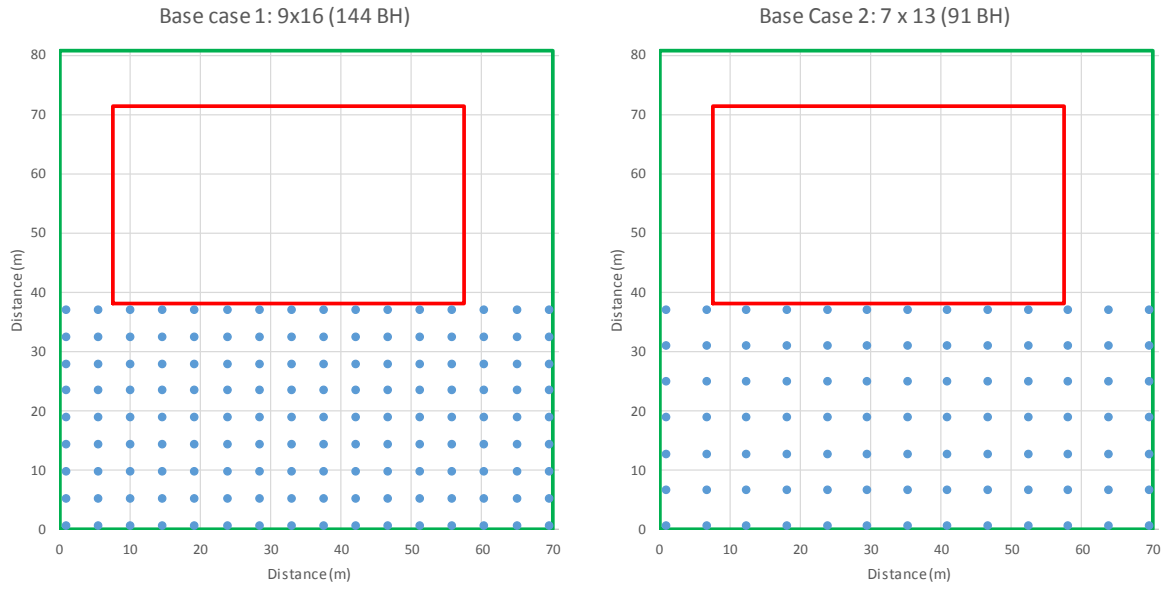

Figure 5. Building footprint in the boundary of the property and the two base cases

The sensitivity of the design of the base case rectangular grid to borehole spacing was analyzed in two different ways. First, keeping the same footprint, a series of rectangular grids with fewer boreholes were sized. The grids had different spacing in the N-S and E-W directions in order to fill the available space. In order to characterize the spacing with one measure, the geometric mean was taken:

$$x_{mean} = \sqrt{x_{NS} \cdot x_{EW}} \tag{1}$$

where x_{NS} and x_{EW} are the spacings in the north-south and east-west directions, respectively.

The results are summarized in Table 1 below. The borehole depths do not include the 2 m assumed burial depth, but the total drilling amount includes this. A common recommendation is to space boreholes 6.1 m (20 ft) apart. The last row of Table 1 shows a case (Base Case 2) where this is approached and, indeed, the savings in total drilling required is 22.5%. But, this comes at the expense of increasing the borehole depth to 135 m. Borehole depth may be constrained due to geological conditions, economics, or a combination of the two. So, it is not always possible to simply increase the spacing and decrease the number of boreholes.

As can be seen from Fig. 6, using fewer boreholes in the same footprint requires deeper boreholes, but the total amount of drilling is reduced. This is consistent with the results reported by Liu et al. (2019). Because it is not always possible or economically feasible to increase the drilling depth, we have defined the two base cases: Base Case 1 with a borehole depth of 110.1 m, and Base Case 2 with a borehole depth of 135 m.

Table 1. Sensitivity of bore field design to borehole spacing when footprint is fixed

# BH in E-W direction	# BH in N-S direction	Spacing in E-W direction (m)	Spacing in N-S direction (m)	Geometric mean spacing (m)	Borehole depth (m)	Total drilling (m)	Savings from Base Case 1
9	16	4.57	4.57	4.57	110.1	16141	-
9	15	4.57	4.90	4.73	113.9	15647	3.0%
9	14	4.57	5.28	4.91	117.7	15081	6.5%
8	15	5.23	4.90	5.06	120.1	14655	9.1%
8	14	5.23	5.28	5.25	123.0	14003	13.1%
8	13	5.23	5.72	5.46	126.1	13323	17.3%
7	13	6.10	5.72	5.90	135.0	12465	22.5%

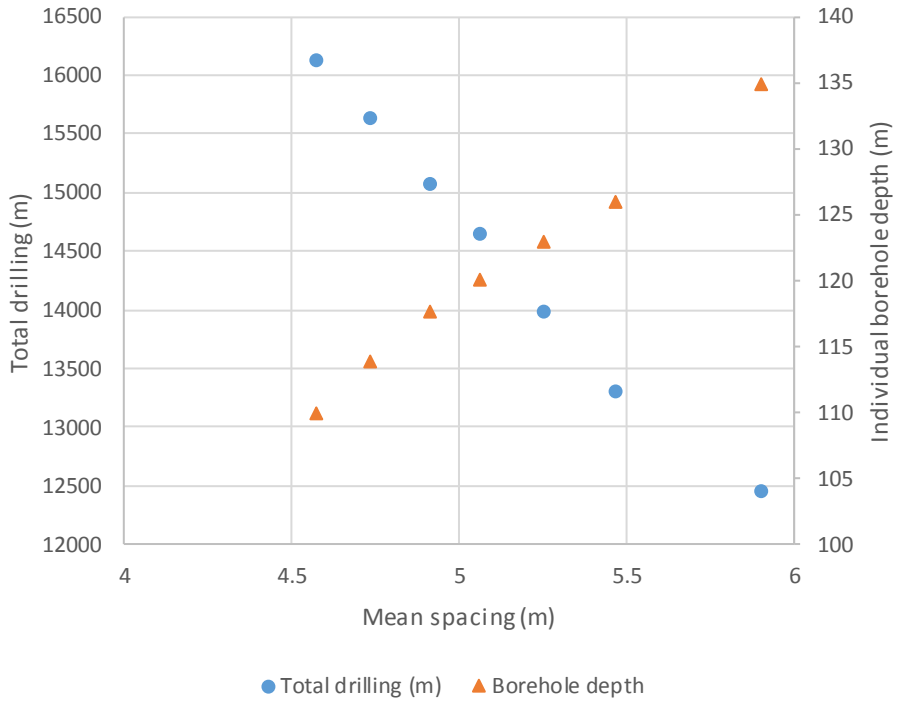

Figure 6. Sensitivity of bore field design to borehole spacing when footprint is fixed.

A second analysis was performed to look at the sensitivity of the design to the spacing when the number of boreholes and configuration (9x16 rectangle) are kept the same, but where the footprint is expanded as the spacing increases. Note that, given the property constraints, it is not possible to expand the footprint of the rectangular grid without drilling boreholes beneath the building. The results are summarized in Table 2 and Fig. 7.

Table 2. Sensitivity of design to spacing when footprint is not constrained.

# BH in E-W direction	# BH in N-S direction	Spacing (m)	Borehole depth (m)	Total drilling (m)	Savings from base case
9	16	4.57	110.1	16141	0.0%
9	16	4.88	102.8	15086	6.5%
9	16	5.18	97.1	14267	11.6%
9	16	5.49	91.2	13424	16.8%
9	16	5.79	87.4	12868	20.3%
9	16	6.10	84.0	12389	23.2%

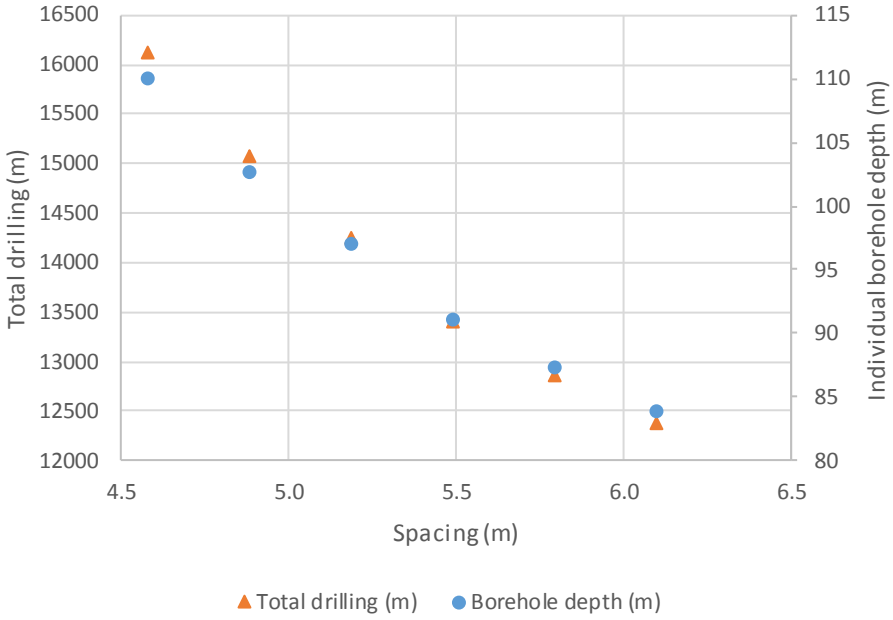

Figure 7. Sensitivity of bore field design to borehole spacing when footprint is not constrained.

The maximum savings cases have roughly the same geometric mean spacing --5.90 m and 6.10 m for the fixed footprint and unconstrained footprint cases, respectively. Interestingly, they also have roughly the same savings in total required drilling length – 22.5% and 23.2%, respectively.

The above cases all make use of a regular grid – that is, the spacing between boreholes is fixed in each direction, though the spacing in the two directions may be different. The use of pygfunction allows other configurations to be examined. Since the borehole-to-borehole interference is stronger for interior boreholes than boreholes on the perimeter, it seems very likely that a strategy that increases the spacing in the interior of the field while decreasing the spacing on the perimeter may be useful. We refer to these bore field configurations as "zoned rectangles". The spacing is constant within the interior zone and within the perimeter zone, but the perimeter zone spacing is less than the interior zone spacing.

A series of six zoned rectangles were analyzed; two cases are shown in Figure 8. The one on the left requires utilizes 116 boreholes of depth 116.2 m, for savings of 15.1% in total drilling depth compared to Base Case 1. Of the zoned rectangles analyzed, this 116-borehole case comes closest to matching the borehole depth of Base Case 1. The configuration on the righthand side of Figure 8 uses 86 boreholes of depth 133.8 m, and so can more fairly be compared to Base Case 2. Compared to Base Case 2, it saves 6.3% in total

drilling depth. In both cases, the zoned rectangle configuration shows noticeable savings compared to a similar regularly spaced rectangular configuration.

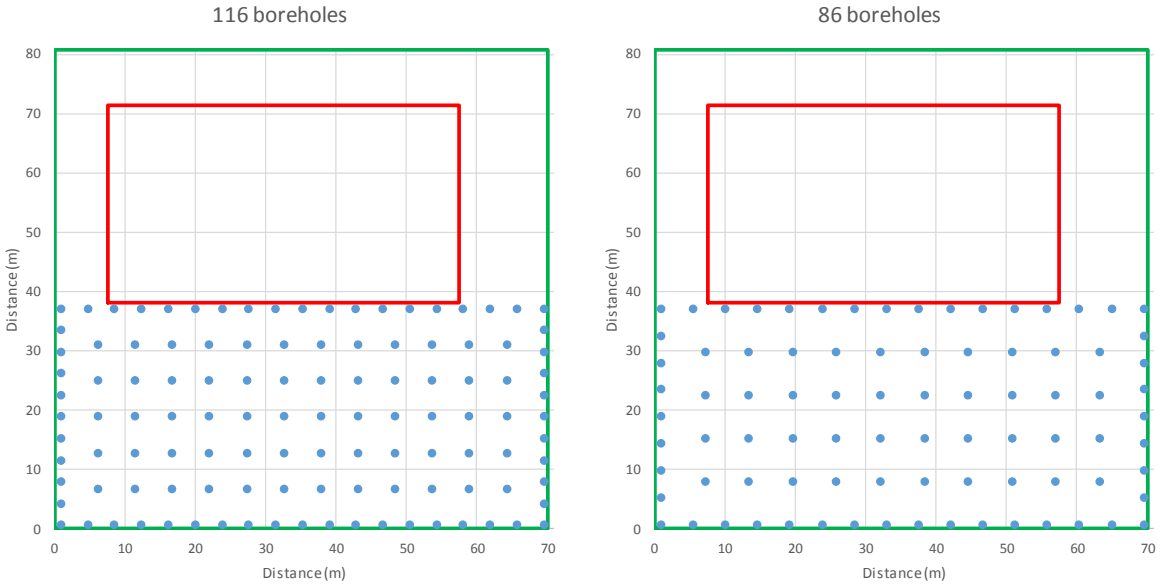

Figure 8. Two "zoned rectangle" bore fields

Having seen that arranging the boreholes differently within the same footprint leads to some significant savings, one may ask how we can take full advantage of the site. There is space all on the north, east, and west sides of the building that is not currently used. And, with current design tools using libraries of g-functions that don't contain suitable configurations, such a design can't be sized with existing design tools.

We generated several "wrap-around" configurations that place boreholes around the building. The total number of boreholes was reduced several times in order to try to roughly match the depths of the two base cases. The spacing around the exterior perimeter, interior perimeter and interior of the field were manually adjusted several times. A configuration that roughly matched the Base Case 1 depth is shown on the left-hand side of Figure 9. This configuration has 84 boreholes with a depth of 108.4m. This represents a savings in total drilling depth of 42.6% compared to Base Case 1!

The configuration on the righthand side of Figure 9 has 60 boreholes of depth 134.5 m, and so may be more fairly compared to Base Case 2. It saves 34.3% in drilling depth compared to Base Case 2. In both cases, making use of additional existing land area and strategically varying the spacing among boreholes allows a significant savings in total drilling depth while maintaining roughly the same individual borehole drilling depth.

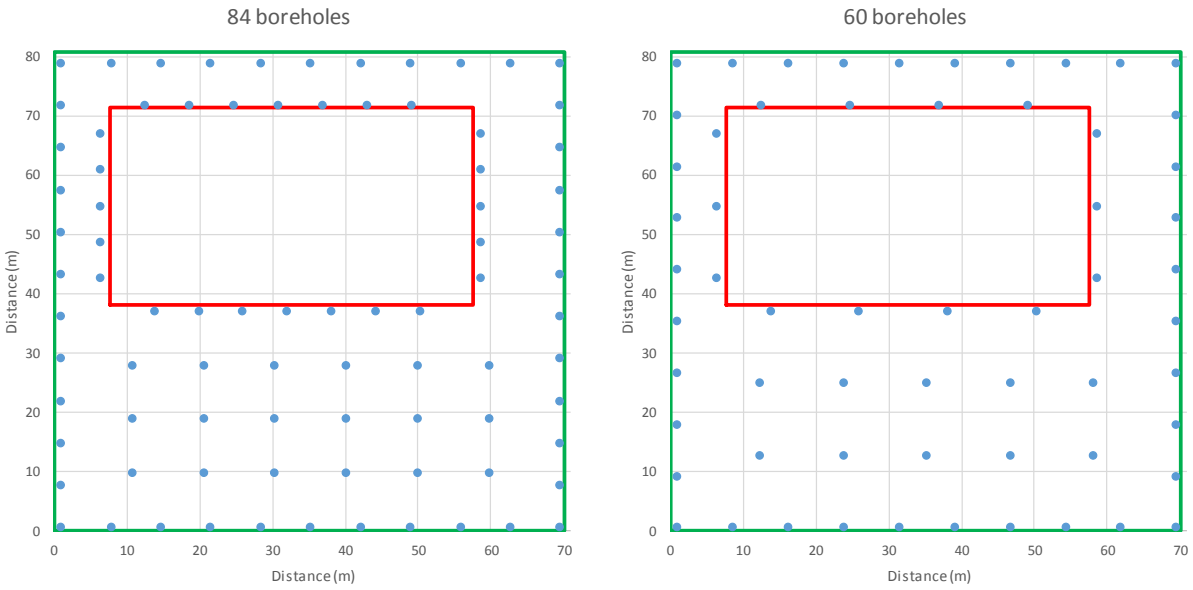

Figure 9. "Wrap-around" ground heat exchanger configurations.

The above comparisons are summarized in Table 3.

Table 3. Summary of Comparisons

Figure	Side	Configuration	# BH	Borehole depth (m)	Total drilling (m)	Comparable Base Case	Savings from Comparable Base Case
4	left	Regular rectangle	144	110.1	16141	1	0%
7	left	Zoned rectangles	116	116.2	13705	1	15.1%
8	left	Wrap-around	84	108.4	9272	1	42.6%
4	right	Regular rectangle	91	135.0	12465	2	0
7	right	Zoned rectangles	86	133.8	11676	2	6.3%
8	right	Wrap-around	60	134.5	8188	2	34.3%

The relationship between the bore field footprint, the number of boreholes, and the bore field configuration is illustrated in Figure 10. In Figure 10, the total drilling depth for each configuration analyzed is plotted as a function of required borehole depth. The zoned rectangles show a clear reduction compared to the regular rectangular configuration over the range of depths analyzed. These configurations utilize the same footprint, but a notable savings is obtained with the zoned rectangles configuration. Even better results are obtained with the wrap-around configurations, which use a larger footprint by placing boreholes on all sides of the building.

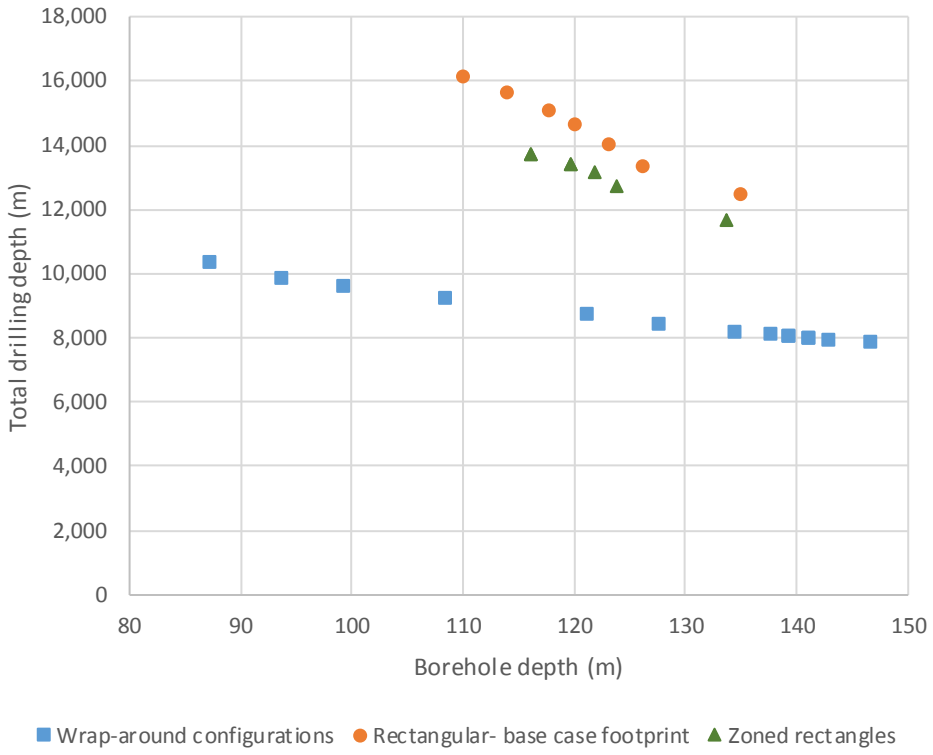

Figure 10. Required total drilling depth for each configuration as a function of required borehole depth

How can these differences be explained? The larger footprint means significantly less borehole-to-borehole thermal interference and less heat saturation in the interior boreholes. One way of quantifying this is to use intermediate results from the g-function calculations. In these calculations, a constant heat input is imposed on the bore field and, in the finite line source superposition, the heat input to each borehole segment is adjusted to give a uniform borehole wall temperature. We have taken the heat input for each borehole at the 20th year, and divided that by the average borehole heat input of the entire bore field. These results are illustrated in Figure 11. For the Base Case 1 configuration shown on the left hand side of Figure 11, the saturation of the interior boreholes is clearly shown by the dark colors for these boreholes. The corner boreholes have around three times the average heat transfer rate; the other perimeter boreholes have around two times the average heat transfer rate, and all the interior boreholes have below-average heat transfer rates. By comparison, the wrap-around configuration with 84 boreholes, 108.4 m deep, shown on the righthand side of Figure 11 has much more uniform heat transfer rates. This can be interpreted as all of the boreholes being more effective over the long term.

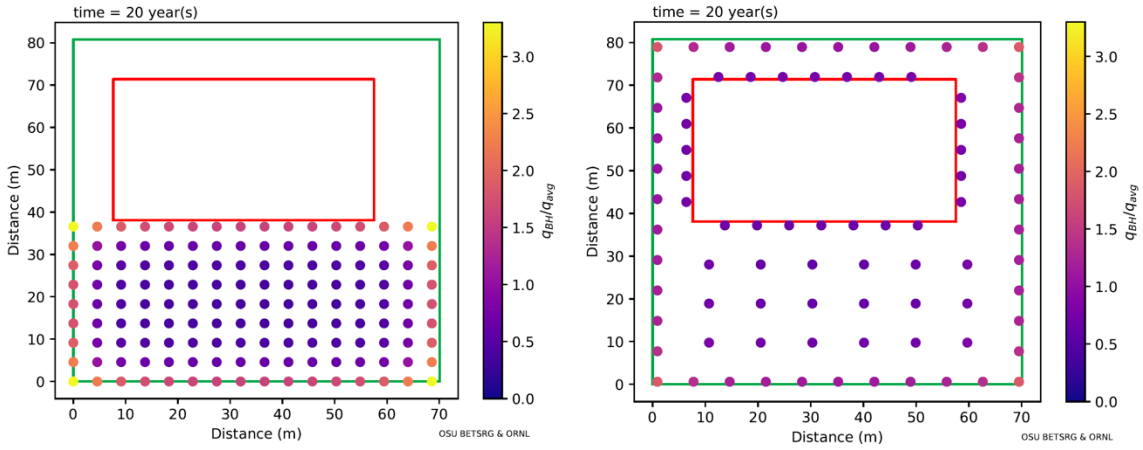

Figure 11. Distribution of heat input to various boreholes in two different bore fields.

But, does this effectiveness translate into better energy efficiency? The two designs shown in Figure 11, Base Case 1 and the 84-borehole wrap-around configuration with 110.1 m and 108.4 m deep boreholes respectively, were simulated for a 20-year period. The building heating and cooling loads for a one-year period were assumed to repeat for 20 years. The heat pump entering fluid

temperatures were calculated for each ground heat exchanger and these temperatures were used with a simple equation fit model of the heat pump performance to determine the required hourly electrical energy.

The heat pump entering fluid temperatures rise over time for both ground heat exchangers. Figure 12 shows the hourly heat pump entering fluid temperatures in July of the 1st year (left) and July of the 20th year (right). As can be seen, in the first year, before the interior of the 144-borehole field is heat saturated, it has lower temperatures. But, over time, the heat pump entering fluid temperatures increase for both fields, but more so for the 144-borehole field. It may also be noted that the 84-borehole field generally has higher diurnal temperature swings. This can be attributed to the considerably lower total length of the boreholes and accordingly higher load per unit length. In turn, the average heat pump entering fluid temperature is lower for the 144-borehole field than the 84-borehole field in the first years of operation, but higher in the later years.

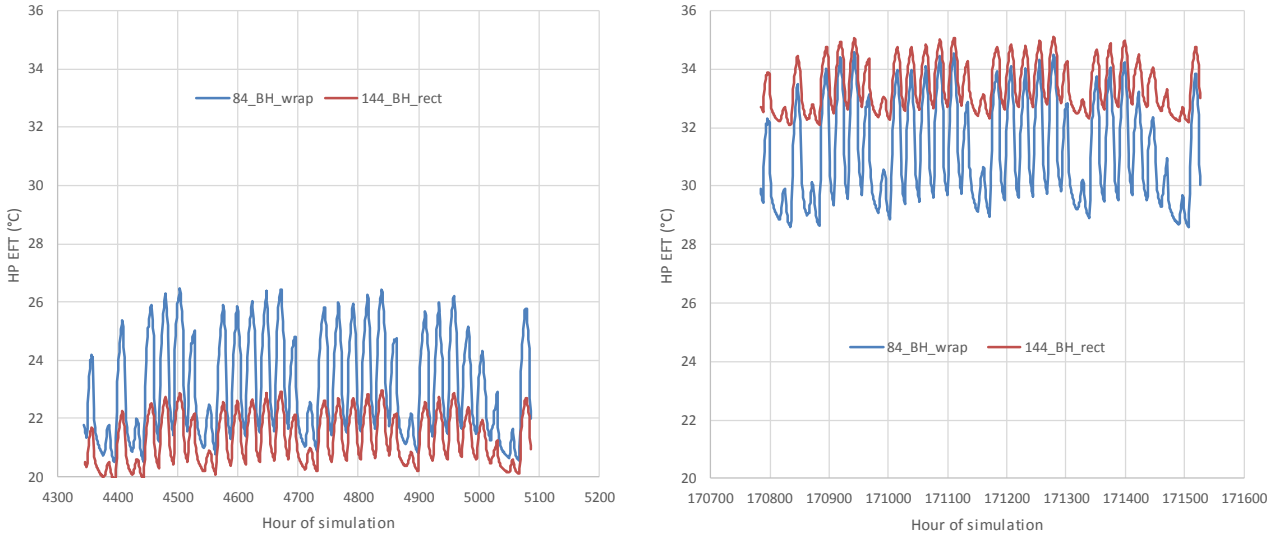

Figure 12. Heat pump entering fluid temperatures in July of the 1st year (left) and 20th year (right)

Figure 13 (left) shows the average annual heat pump entering fluid temperatures; the 144-borehole field quickly increases beyond the 84-borehole field. This difference in temperatures as a moderate impact on the electricity consumption of the two systems. While the 84-borehole field starts with slightly higher annual electricity consumption, it is surpassed after a few years by the 144-borehole field. Over the 20-year analysis period, the heat pump served by the 144-borehole field uses about 2.3% more electricity and in the 20th year, it uses 5.4% more electricity. This analysis neglects pumping energy, cycling-losses, and some 2nd-order effects, but the 84-borehole field should give superior performance if other aspects of the design are carefully treated.

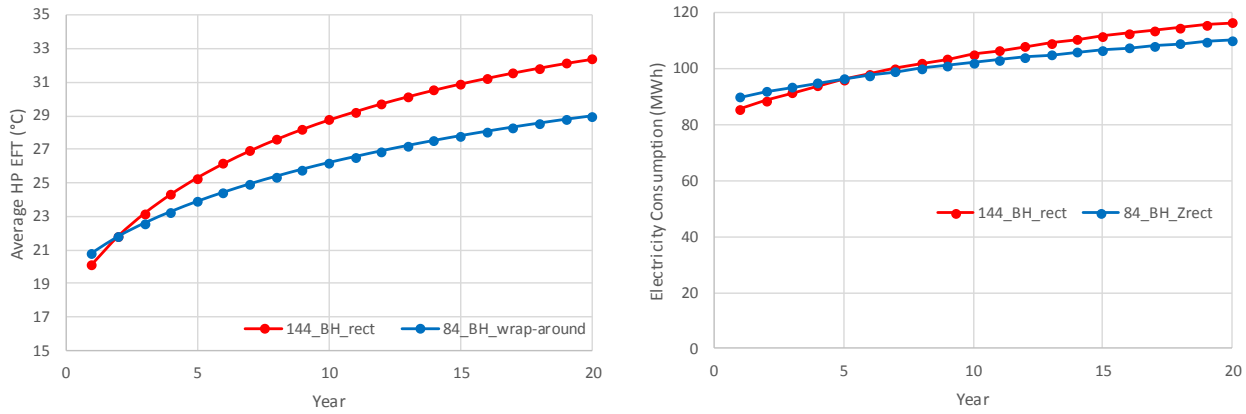

Figure 13. Annual average heat pump entering fluid temperatures (left) and electricity consumption (right)

4. DISCUSSION AND CONCLUSIONS

Alternative designs of bore field that utilize all the available land and strategically place boreholes with different spacing at perimeter and inner zones can significantly reduce the total length of a bore field while retaining the same performance. It thus has potential to drastically reduce the cost of VBGHE and make GSHP systems more economically competitive. While it has been understood for some time that increasing the spacing of boreholes can reduce the total required drilling, there have been few papers that have addressed the

use of irregularly spaced boreholes to optimize the VBGHE design other than Bayer, et al. (2015). Furthermore, the tools needed to quantify this have not been widely available until Cimmino (2019b) released pygfunction.

A case study of a medium-size office building in Atlanta shows that this strategy is very effective when the heat extraction and heat rejection imposed to a bore field are significantly imbalanced on an annual basis and when additional space to place some boreholes was available around the perimeter of the office building. As demonstrated in this paper, culminating in Figure 10, increasing the spacing between boreholes allows a reduction in the total drilling length, but at the expense of deeper individual boreholes. As the cost for drilling deeper may increase nonlinearly, and site conditions may limit the depth of the boreholes, it is probably fairest to compare regularly spaced configurations and irregularly spaced configurations with similar borehole depths.

Comparing the alternative 84-borehole wrap-around configuration to the 144-borehole regularly spaced rectangular configuration (Base Case 1), with borehole depths of 108.4 m and 110.1 m, respectively, the total savings in drilling length was 42.6%. Comparing the alternative 60-borehole wrap-around configuration to the 91-borehole regularly spaced rectangular configuration (Base Case 2), with borehole depths of 135m and 134.5 m, respectively, the total savings in drilling length was 34.3%. These savings are quite significant. Furthermore, an analysis of the energy consumed by the heat pumps showed savings on the order of 2% over the 20-year design period for the wrap-around configuration.

Further research is needed to investigate other possible strategies such as utilizing ground heat exchangers with boreholes of different depths. Investigation of using angled boreholes is also needed, though pygfunction does not currently support calculation of g-functions for boreholes that are not vertical.

Further research and development is needed to develop optimization algorithms and software that can determine the most cost-effective bore field design for a given building based on the size and shape of the available land area for drilling boreholes.

ACKNOWLEDGMENTS

This material is based upon work supported by the U.S. Department of Energy's Office of Energy Efficiency and Renewable Energy (EERE), under the Geothermal Technologies Office, Low-Temperature and Co-Produced Resources Program. The authors would like to thank Dr. Massimo Cimmino – without his development of the open-source pygfunction, this work would not have been possible. The authors also appreciate the guidance and inputs of Mrs. Arlene Anderson, the Lead Technology Manager of Low-Temperature Geothermal Program at U.S. Department of Energy.

REFERENCES

Bayer P., M. de Paly, M. Beck 2014. Strategic optimization of borehole heat exchanger field for seasonal geothermal heating and cooling, *Applied Energy* 136 (2014) 445–453

BLOCON 2019. EED version 4 Update manual.

Cimmino, M. 2019a. Semi-Analytical Method for g-Function Calculation of bore fields with series- and parallel-connected boreholes. Science and Technology for the Built Environment 25(8): 1007-1022.

Cimmino, M. 2019b. "pygfunction GitHub Page." Retrieved October 24, 2019, from https://github.com/MassimoCimmino/pygfunction.

Cimmino, M. and M. Bernier. 2014. A semi-analytical method to generate g-functions for geothermal bore fields. *International Journal of Heat and Mass Transfer* 70: 641-650.

Claesson, J. and P. Eskilson. 1985. Thermal analysis of heat extraction boreholes. Proceedings of 3rd International Conference on Energy Storage for Building Heating and Cooling. *Proceedings*, ENERSTOCK 85, Toronto, Canada, Public Works Canada. 222–227.

Claesson, J. and S. Javed. 2011. An Analytical Method to Calculate Borehole Fluid Temperatures for Time-scales from Minutes to Decades. *ASHRAE Transactions* 117(2): 279-288.

Cullin, J. R. and J. D. Spitler. 2011. A computationally efficient hybrid time step methodology for simulation of ground heat exchangers. *Geothermics* 40(2): 144-156.

D&R International. 2012. 2011 Buildings Energy Data Book. Prepared for the Buildings Technologies Program, Energy Efficiency and Renewable Energy, U.S. Department of Energy.

Deru, M., K. Field, D. Studer, K. Benne, B. Griffith, P. A. Torcellini, B. Liu, M. Halverson, D. Winiarski, M. Rosenberg, M. Yazdanian, J. Huang and D. Crawley 2011. U.S. Department of Energy Commercial Reference Building Models of the National Building Stock. NREL, NREL/TP-5500-46861.

Eskilson, P. 1986. Superposition Borehole Model: Manual for Computer Code. University of Lund.

Liu, X., Y. Polsky, D. Qian and J. Mcdonald. 2018. Analysis of Cost Reduction Potential of Vertical Bore Ground Heat Exchanger. ORNL/TM-2018/756. Oak Ridge, TN: Oak Ridge National Laboratory.

Liu, X., P. Hughes, K. McCabe, J. Spitler, and L. Southard. 2019. GeoVision Analysis Supporting Task Force Report: Thermal Applications—Geothermal Heat Pumps. ORNL/TM-2019/502. Oak Ridge, TN: Oak Ridge National Laboratory.

Mitchell, M. S. and J. D. Spitler. 2019. Characterization, testing, and optimization of load aggregation methods for ground heat exchanger response-factor models. *Science and Technology for the Built Environment* 25(8): 1036-1051.

NYSERDA (New York State Energy Research and Development Authority). 2017. Renewable Heating and Cooling Policy Framework. (Available at https://www.nyserda.ny.gov/-/media/Files/Publications/PPSER/NYSERDA/RHC-Framework.pdf)

OSU 2016. GLHEPro 5.0 for Windows - Users' Guide. Stillwater.

Spitler, J. D. 2000. GLHEPRO - A Design Tool for Commercial Building Ground Loop Heat Exchangers. Fourth International Heat Pumps in Cold Climates Conference, Aylmer, Québec.

Spitler, J. D. and J. C. Cook 2019. Evaluation of Recent Developments in Ground Heat Exchanger Modeling. Oklahoma State University.

Xu, X. and J. D. Spitler. 2006. Modelling of Vertical Ground Loop Heat Exchangers with Variable Convective Resistance and Thermal Mass of the Fluid. *Proceedings*, 10th International Conference on Thermal Energy Storage - Ecostock 2006, Pomona, NJ. 8.